Journal of Mammalian Evolution
https://doi.org/10.1007/s10914-021-09545-w

ORIGINAL PAPER

# The Early Eocene Climatic Optimum at the Lower Section of the Lumbrera Formation (Ypresian, Salta Province, Northwestern Argentina): Origin and Early Diversification of the Cingulata

**Juan Carlos Fernicola[1,2,3] · Ana N. Zimicz[1,4] · Laura Chornogubsky[1,2] · Mihai Ducea[5,6] · Laura E. Cruz[1,2] · Mariano Bond[1,7] · Michelle Arnal[1,8] · Magalí Cárdenas[1,2] · Mercedes Fernández[1,2,3]**

Received: 28 August 2020 / Accepted: 29 March 2021


## Abstract

Recently, the basal beds of the lower section of the Lumbrera Formation have been referred to the early Eocene (Ypresian) based on the identification of a succession of hyperthermal events globally dated between 52 and 55 Ma. Nevertheless, this section have also been referred to the middle Eocene (Lutetian) based on the 'evolutionary stage' of its fossil mammals. In this contribution, we present a new $^{238}U$-$^{206}Pb$ isochron age (46.2 Ma) obtained from samples taken on various independent points across paleosol and matrix positioned at the top of the lower section of the Lumbrera Formation. The new age is consistent with the hyperthermal scheme and constrains the deposition of the lower section of the Lumbrera Fm. between 55–46.2 Ma. In this new geochronological framework, we present one of the most ancient cingulate assemblages from America, recorded during the early Eocene hyperthermal. The specimens involved were recovered from the lowest levels of the lower section of the Lumbrera Formation at Los Cardones National Park, Calchaquí Valleys, Salta Province, Argentina. This cingulate assemblage is formed by the armadillos *Pucatherium parvum*, a species widely distributed in the Eocene of northwestern Argentina and a new taxon, *Noatherium emilioi*, gen. et sp. nov. In this new geochronological framework, the taxonomic composition and morphological variations observed in the two species described here and their probably contemporaneous *Riostegotherium yanei* from the Itaboraí basin (Brazil) support an early diversification of the Cingulata during the Paleocene, and reinforce an intertropical origin for the group.

**Keywords** Mammals · Cingulates · Lower section of the Lumbrera formation · Northwestern Argentina · Paleogene · Eocene

## Introduction

Xenarthra represents one of the four early diverging natural groups of placental mammals (Meredith et al. 2011); recent molecular studies estimated its time of divergence by the end of the Cretaceous (Meredith et al. 2011; Delsuc et al. 2012, 2016; Gibb et al. 2016). This group includes the Folivora (terrestrial and arboreal sloths), Vermilingua (anteaters), and Cingulata (extinct and extant armadillos, glyptodonts, pampatheres, and horned peltephilines), and

✉ Juan Carlos Fernicola
jctano@yahoo.com

[1] Consejo Nacional de Investigaciones Científicas y Técnicas, Conicet, Argentina

[2] Museo Argentino de Ciencias Naturales 'Bernardino Rivadavia', Av. Ángel Gallardo 470, 1405 Ciudad Autónoma de Buenos Aires, Argentina

[3] Departamento de Ciencias Básicas, Universidad Nacional de Luján (UNLu), Ruta 5 y Avenida Constitución (6700), Luján, Buenos Aires, Argentina

[4] Instituto de Bio y Geociencias del Noroeste Argentino, Av. Bolivia 5550, 4400 Salta, Argentina

[5] Department of Geosciences, University of Arizona, 85721 Tucson, AZ, USA

[6] Faculty of Geology and Geophysics, University of Bucharest, Bucharest, Romania

[7] División Paleontología Vertebrados, Museo de La Plata, Facultad de Ciencias Naturales y Museo, UNLP, Paseo del Bosque s/n, B1900FWA, La Plata, Argentina

[8] División Paleontología Vertebrados, Facultad de Ciencias Naturales y Museo, Unidades de Investigación Anexo Museo de La Plata, UNLP, Av. 122 y 60, B1900FWA, La Plata, Argentina

Published online: 10 May 2021

it represents one of the most bizarre clades of all known mammals, with its most distinctive character being the presence of a supplementary intervertebral joint in the vertebrae after the diaphragm (Gaudin 1999), called xenarthrous articulations, from which the group gets its name. Another unique feature among placental mammals that is observed in the Xenarthra is the presence of osteoderms. These dermal ossicles are absent in anteaters and restricted to only a few genera of sloths (Mc Donald 2018). In Cingulata, they form a large dorsal carapace composed of hundreds of articulated osteoderms, covered with epidermal scales, which, together with those present in the shields that cover the head and tail, considerably enhance the fossilization potential of these animals. This is clearly seen in the fact that most of the fossil taxa erected since the 19th century are based on osteoderms (Fernicola and Porpino 2012).

Until now, the oldest record of cingulates corresponds to the armadillo *Riostegotherium yanei* Oliveira and Berqvist, 1998, based on osteoderms collected in the Itaboraí Formation at the Itaboraí Basin of Brazil (Oliveira and Bergqvist 1998; Bergqvist et al. 2019) with an estimated age of ca. 53 Ma (early Eocene, Ypresian) (Oliveira and Bergqvist 1998; Woodburne et al. 2014). Subsequent cingulate records have been reported from younger levels in the early and middle Eocene of the Argentinean Patagonia (e.g., Carlini et al. 2010; Ciancio et al. 2016; Tejedor et al. 2009). The oldest cingulates described for the northwest region of Argentina were recovered from the lower section of the Lumbrera Formation, and together with the remaining fossil mammals (García-López et al. 2019; Fernández et al. 2021), these were confronted with those described for the Vacan Subage (middle Eocene, Lutetian) of the Casamayoran SALMA (Powell et al. 2011; Herrera et al. 2016). This confrontation was based on the idea of a similar 'evolutionary stage' between the fossil mammal assemblage recovered from levels of the Lumbrera Formation and that of the Casamayoran SALMA in Patagonia (Carbajal et al. 1977; Pascual 1980a, b, 1981; Bond and Vucetich 1983). However, this biochronological model was recently questioned by Andrews et al. (2017). These authors, based on the study of the carbon isotope in paleosols of the Paleocene sequence of the Mealla, Maíz Gordo, and lower section of the Lumbrera formations, recognized a hyperthermal sequence in which the last unit was deposited during the early Eocene (52–55 Ma).

In this contribution, we present a new dating, which was taken from the top of the lower section of the Lumbrera Formation at the Tres Cruces section (Jujuy Province). This allows us to evaluate the chronology previously proposed for this formation. In this context, we analyzed a new armadillo assemblage composed of two different genera and species based on specimens collected by us from the base of the lower section of the Lumbrera Formation. Finally, the taxonomic composition and morphological variation observed in the two taxa recognized in this association and those that are contemporaneous allow us to discuss the time of diversification of the Cingulata.

## Materials and Methods

The cingulate specimens studied here were collected between the years 2017 and 2018 by our team from the basal levels of the lower section of the Lumbrera Formation (LSLF) (Santa Bárbara subgroup; Salta Group), exposed at the southern margin of the Tin Tin range, from 100 m above the boundary with the Maíz Gordo Formation (Fm.) (Fig. 1). These specimens are deposited at the Paleontology Collection of the Instituto de Bio y Geociencias del NoroesteArgentino (IBIGEO), Rosario de Lerma, Salta Province, Argentina. The materials were identified through comparison with the type and referred specimens housed at different institutions, Museo de La Plata, Instituto Miguel Lillo, and Museo Argentino de Ciencias Naturales 'Bernardino Rivadavia'. The specimens are identified with their repository number when first mentioned in the text.

Comparison of the taxonomic richness among the localities whose levels were assigned to the time lapse between 52 and 56 Ma (early Eocene, Ypresian) is based on the presence or absence of each taxon listed in each locality. Unfortunately, we do not have the precise information about the stratigraphic position of the only cingulate, *Lumbreratherium oblitum* Herrera et al., 2016, recognized until today in the lower section of the Lumbrera Fm. (LSLF) at Pampa Grande, Salta Province (Herrera et al. 2016). Because the LSLF involves a time span of around 7 Ma, and given the lack of stratigraphic provenance for *L. oblitum*, we can not undoubtedly assign this taxon to the early Eocene. Therefore, it is not possible to assign without doubt this taxon to the mentioned temporal range.

Osteoderms were measured with a Vernier digital caliper (+/- 0.001 mm). The photographs were taken with a Canon EOS Rebel SL2 camera.

The descriptive terminology follows Fernicola and Vizcaíno (2008, 2019), Krmpotic et al. (2009), Ciancio et al. (2013), and Francia and Ciancio (2013) (Fig. 2).

### Geochronology: Sampling and Analytical Methods

In the present study, we report a carbonate U-Pb isochron age on samples from the top of the LSLF at the Tres Cruces section (Jujuy Province; Fig. 1a). The sample comes from a level at 330 m interbedded in the Faja Verde, a few meters below the contact with the Casa Grande Fm. (Fig. 1c). The isotopic ratios were measured on whole rock samples representing various

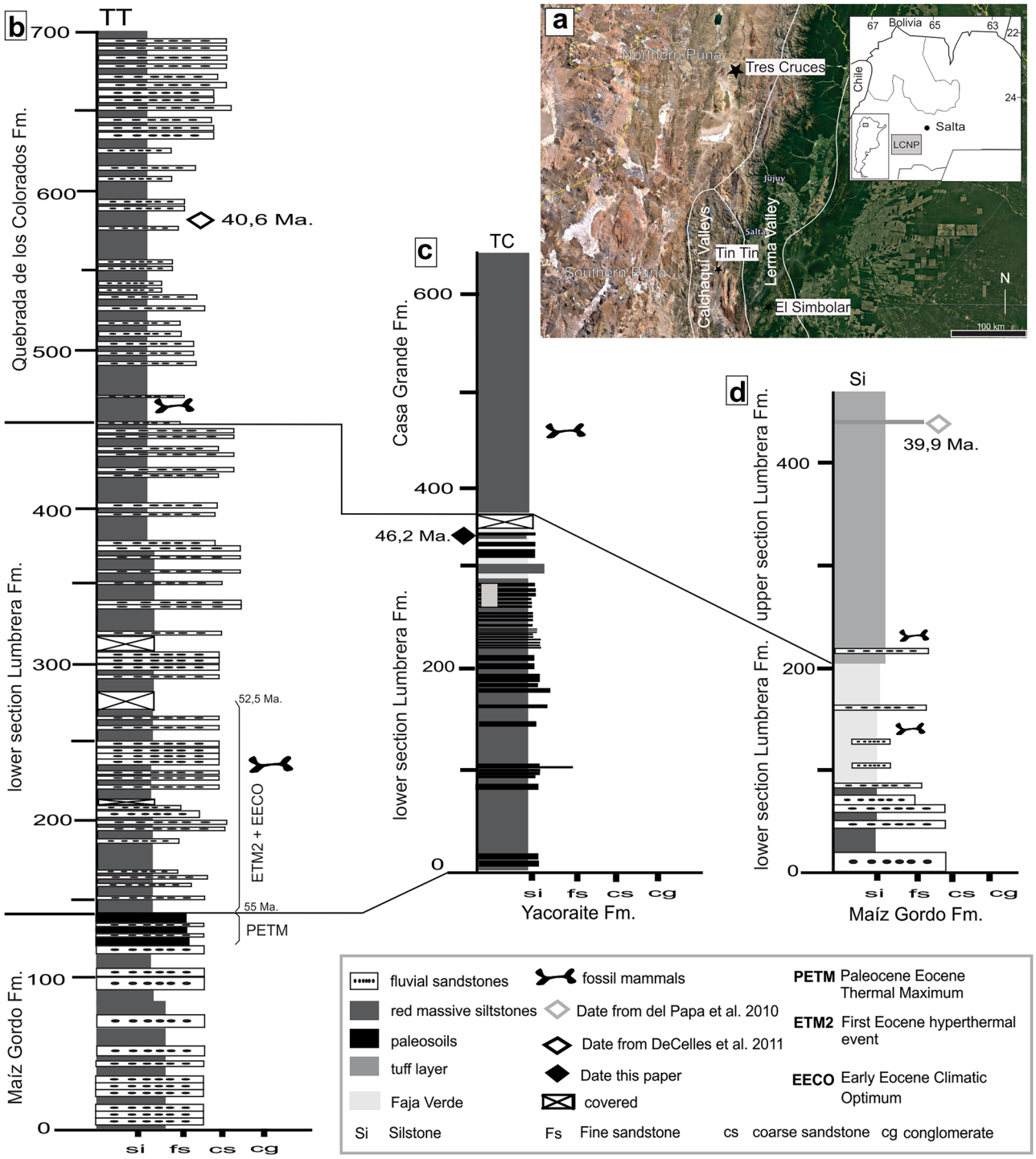


**Fig. 1** Locality and stratigraphy of the studied area. (**a**) Geographic location of the study area; (**b**) Sedimentary log of the Maíz Gordo, lower section of the Lumbrera, and Quebrada de Los Colorados formations at Tin Tin (TT) locality, Los Cardones National Park, Salta Province, Argentina, modified after DeCelles et al. (2011); (**c**) Sedimentary log of the lower section of the Lumbrera, and Casa Grande formations at Tres Cruces (TC), Jujuy Province, Argentina, modified after DeCelles et al. (2011); (**d**) Sedimentary levels of the lower and upper sections of the Lumbrera Fm. at El Simbolar (Si), Salta Province, Argentina, modified from Del Papa et al. (2010). Age for LSLF based on sample LSLF-ELF1 (this paper). Age for QLCF after DeCelles et al. (2011). Age of the USLF after del Papa et al. (2010). PETM, ETM2, and EECO location after Andrews et al. (2017)

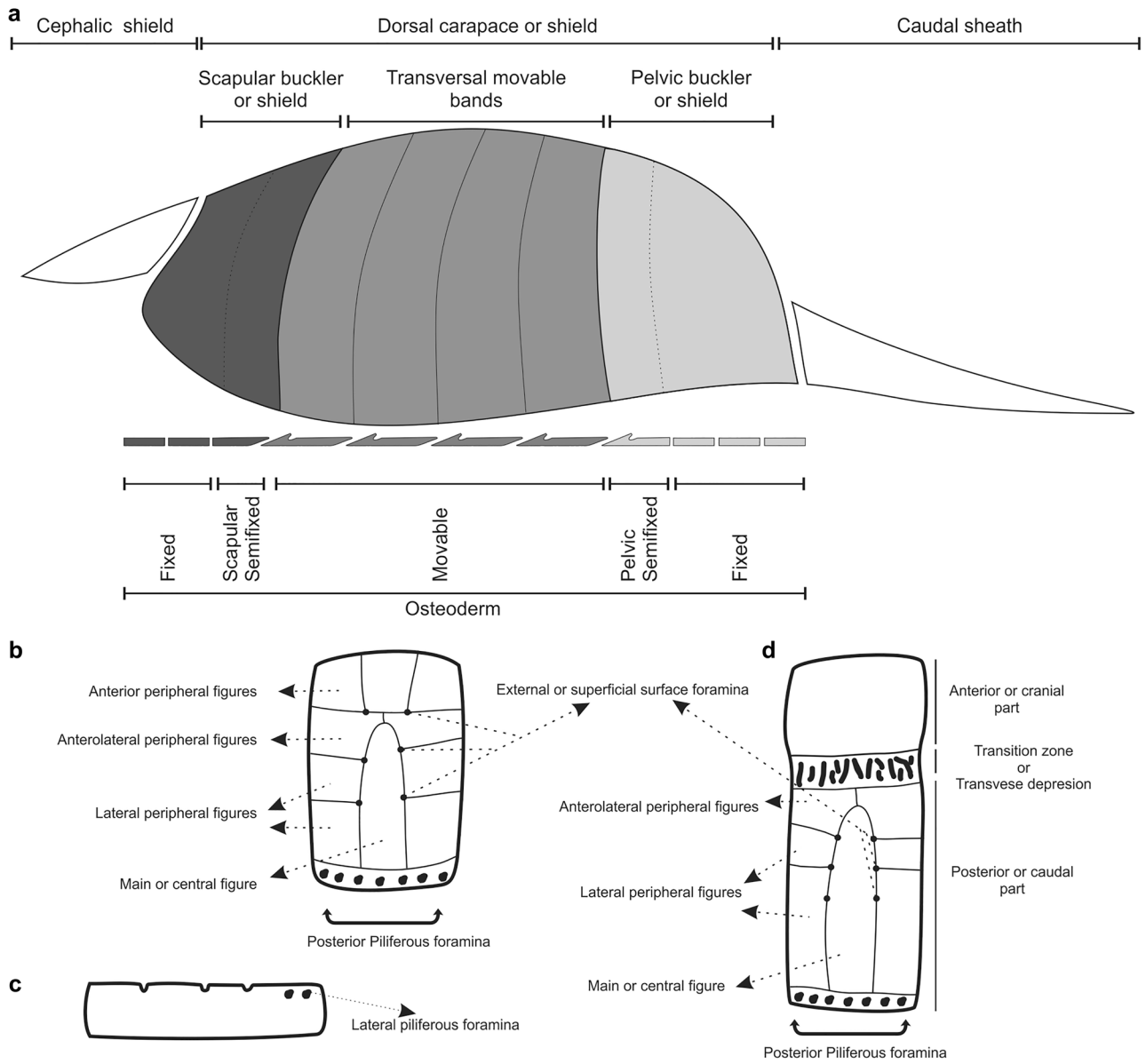


**Fig. 2** Terminology of the dorsal carapace and osteoderm features used in the text. (**a**) Section of the dorsal carapace and position of the osteoderms; (**b**) External surface of the fixed osteoderm; (**c**) Lateral surface of the fixed osteoderm; (**d**) External surface of the movable osteoderm

independent points across paleosol and matrix. Zones of different coloration were used here as markers for individual data points. The samples were extracted via a Micromill instrument (Ducea et al. 2003), which has a spatial resolution of a few (< 10) microns, and a powder recovery rate of > 90%. Rock powders were put in large Savillex vials and dissolved in hot 2 M HNO3.

U-Pb ages were determined in solution on a high-resolution ISOPROBE multi-collector ICP-MS instrument at the Department of Geosciences of the University of Arizona (USA). After dissolution, miniaturized cation columns were used to separate and discard the Ca-rich fraction, which commonly clogs the instrument cones. Analysis routine involved 30 individual measurements, at about one measurement per second. Matheson ultrapure Ar gas was used and monitored Hg interferences at mass 202. A correction was then applied to $^{204}$Pb. The $^{238}$U/$^{204}$Pb, $^{206}$Pb/$^{204}$Pb, $^{207}$Pb/$^{204}$Pb, and $^{208}$Pb/$^{204}$Pb fractionations were corrected using two external standards, glass NBS981 and carbonate standard MACS-3. Standards were analyzed throughout the day in between unknowns, and the unknowns were corrected for fractionation using an internal bracketing technique similar to that used in zircon U-Pb chronology (e.g., Barbeau et al. 2005 for a study performed on this instrument). In addition, it was used an internal carbonate standard and various solutions with U and Pb of concentrations

similar to those in the unknowns. Ages were calculated using the ISOPLOT macro (Ludwig 2012) and we report our age as a $^{238}U/^{204}Pb$ -$^{206}Pb/^{204}Pb$ isochron (Fig. 3), with its estimated error and MSWD.

*Institutional abbreviations*. IBIGEO-P, Instituto de Biología y Geología, Paleontology Collection, Salta Province, Argentina; MACN, Museo Argentino de Ciencias Naturales 'Bernardino Rivadavia', Ciudad Autónoma de Buenos Aires, Argentina; MLP, Museo de La Plata, Buenos Aires Province, Argentina; PVL, Vertebrate Paleontology Collection of the Instituto Miguel Lillo, Tucumán Province, Argentina.

*Other abbreviations*. EECO, Early Eocene Climatic Optimum; ETM2, Eocene Thermal Maximum 2; Fm., Formation; LCNP, Los Cardones National Park; LSLF, Lower section of the Lumbrera Formation; Ma, mega-annum, one million years in the radioisotopic time scale; NWA, Northwestern Argentina; PETM, Paleocene-Eocene Thermal Maximum; QLCF, Quebrada de Los Colorados Formation; SALMA, South American Land Mammal Age; USLF, Upper section of the Lumbrera Formation.

The datasets generated and/or analyzed during the current study are available from the corresponding author on reasonable request.

## Geological Setting

The materials described here were collected from the outcrops of the basal levels of the LSLF exposed at the southern boundary of the Tin Tin range at the Los Cardones National Park (Calchaquí Valleys, Salta Province, NWA) (Fig. 1a).

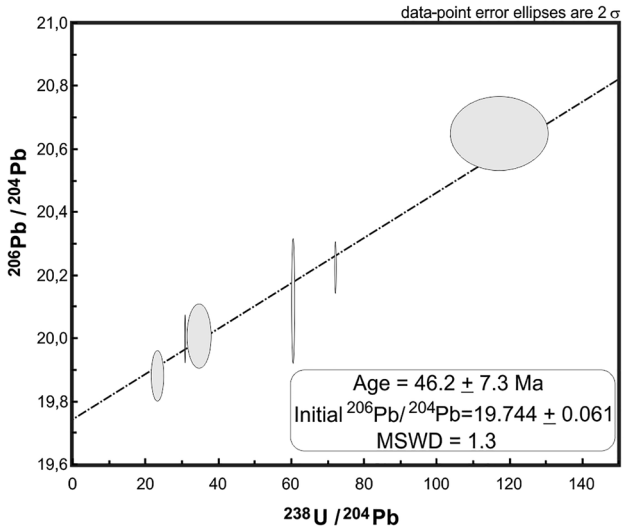


**Fig. 3** $^{206}Pb/^{204}Pb$-$^{238}U/^{204}Pb$ isochron age for six fractions of carbonate material from sample LSLF-ELF1. Individual 2 s errors are shown as ellipses on the isochron. Age, age error and MSWD (1.3) were calculated with ISOPLOT, an excel macro (Ludwig 2012)

The Lumbrera Fm. is divided into the Lower (LSLM) and Upper (USLF) sections (del Papa 2006; del Papa et al. 2010). Only the LSLF outcrops in the study area (DeCelles et al. 2011; del Papa et al. 2013; Andrews et al. 2017) (Fig. 1b). It has an average thickness of 500 m (DeCelles et al. 2011), it unconformably overlies the Maíz Gordo Fm. (Thanetian-early Ypresian) (Andrews et al. 2017), and it is separated from the overlying QLCF (Bartonian) by an erosive discontinuity (del Papa et al. 2013). The LSLF in the study area (Fig. 1a, b) shows different facies associations with respect to the other outcrops in the Puna Plateau (Fig. 1c) in Jujuy Province (del Papa 2006) and Lerma Valley (Fig. 1d). Along the Calchaquí valleys, it is dominated by medium- to fine-grained sandstones interbedded with decimeter-to-meter thick red siltstone, fine-grained sandstone layers, and massive red mudstone with calcareous nodules (Marquillas et al. 2005). These facies associations represent a perennial fluvial system developed along the eastern margin of the basin (del Papa 2006). In the Jujuy Province and Lerma Valley, the fluvial system occurring at the base of the section is transitionally replaced to the top by a lacustrine deposit known as 'Faja Verde' (del Papa 2006; DeCelles et al. 2011). This deposit consists of dark green to gray laminated claystone and sheet-like, fine sandstone and stromatolite (Fig. 1c, d).

The age of the whole Lumbrera Fm. has been strongly debated, especially concerning the base of the unit. The top of the formation is constrained by a U/Pb zircon age of 39.9 Ma (del Papa et al. 2010) on the uppermost levels of the USLF. However, the absence of radioisotopic data for the underlying Maíz Gordo Fm., and the identification of an internal omission surface separating the lower and upper sections in the Lumbrera Fm. (del Papa et al. 2010) have promoted the discussion about the interval represented by the LSLF. There are three models in the literature concerning the age of the LSLF. First, del Papa et al. (2010) assigned a relative age of 46 Ma (middle Eocene, Lutetian) for the base of the unit based on the stage of evolution of the fossil mammals recovered. Second, Sempere et al. (1997) correlated the LSLF to the magnetic polarity interval between Chron 26n to Chron 24r. This model gives an age of 54.5 Ma for the top of the LSLF (early Eocene, Ypresian). However, the authors mentioned that the paleomagnetic analysis was done in 1977, when laboratory techniques were less rigorous than present so the result was not completely reliable (Sempere et al. 1997: 725). Third, recent magnetostratigraphic studies of the Maíz Gordo Fm. correlated this unit to the magnetic polarity interval between Chron 26n and the base of Chron 24r (Andrews et al. 2017; White et al. 2018). In this last scenario, the LSLF could have been deposited during the early Eocene (Ypresian), and then, the whole Lumbrera Fm. involves a time span of around 14 Ma.

Andrews et al. (2017) reconstructed the PETM event in the Salta basin identifying the thick paleosoils of the top

of the Maíz Gordo Fm. In addition, they found important isotopic excursions in the first 150 m of the LSLF at the Tin Tin section, which corresponds to our fossiliferous levels (Fig. 1b). Andrews et al. (2017) gave two alternative interpretations for these excursions considering the different ages given for the LSLF. One of these interpretations is based on the age model of Sempere et al. (1997), in which the age of the top of the LSLF is 54.5 Ma (early Ypresian). Andrews et al. (2017) correlated the carbon excursions recorded in the LSLF to the early Eocene thermal events identified by Zachos et al. (2001, 2008, 2010) in the oceanic basins. In this scenario, the LSLF registered the EECO and ETM2 (Zachos et al. 2008). The other alternative scenario evaluated by Andrews et al. (2017) is based on the age model of del Papa et al. (2010), in which the base of the LSLF is equivalent to 46 Ma. This implies that the carbon excursions registered in the LSLF represent the middle to late Eocene carbon cycle perturbations. However, Andrews et al. (2017:188) considered this hypothesis less reliable because the carbon excursions during this time are less frequent, show less depletion, and are not well characterized. On this base, the authors conclude that Sempere's model was the best constraint for the age of the LSLF (Andrews et al. 2017: 188; but see below).

## Systematic Paleontology

Xenarthra Cope, 1889
Cingulata Illiger, 1811
Cingulata incertae sedis

*Noatherium*, gen. nov.

**Type Species** *Noatherium emilioi*, gen. et sp. nov.

**Derivation of Name** The generic epithet, *Noatherium*, derives from 'NOA', which is the abbreviation of northwest Argentina in Spanish, name of the Argentinean region where the type locality of this species is located, plus '*therium*', which derives from the Latin word *therion*, which means beast.

**Diagnosis** As for the type species by monotypy.

*Noatherium emilioi*, gen. et sp. nov.
(Fig. 4a-f)

**Holotype** IBIGEO-P 72, one fixed osteoderm.

**Paratypes** IBIGEO-P 74, one semifixed osteoderm of the first row of the pelvic buckler; IBIGEO-P 75, one movable osteoderm.

**Geographic and Stratigraphic Occurrence** Los Cardones National Park, Calchaquí Valleys, Salta Province, Argentina; lower section of the Lumbrera Fm.; Santa Bárbara group.

**Derivation of Name** The specific epithet, *emilioi*, refers to the park ranger Emilio Daher, whose assistance and support allowed us to carry out our fieldwork at Los Cardones National Park, Salta Province, northwestern Argentina.

**Comments** Sintype specimens were recovered at the same level, and very close to each other; although it is highly probable, we cannot confirm that they are part of the same

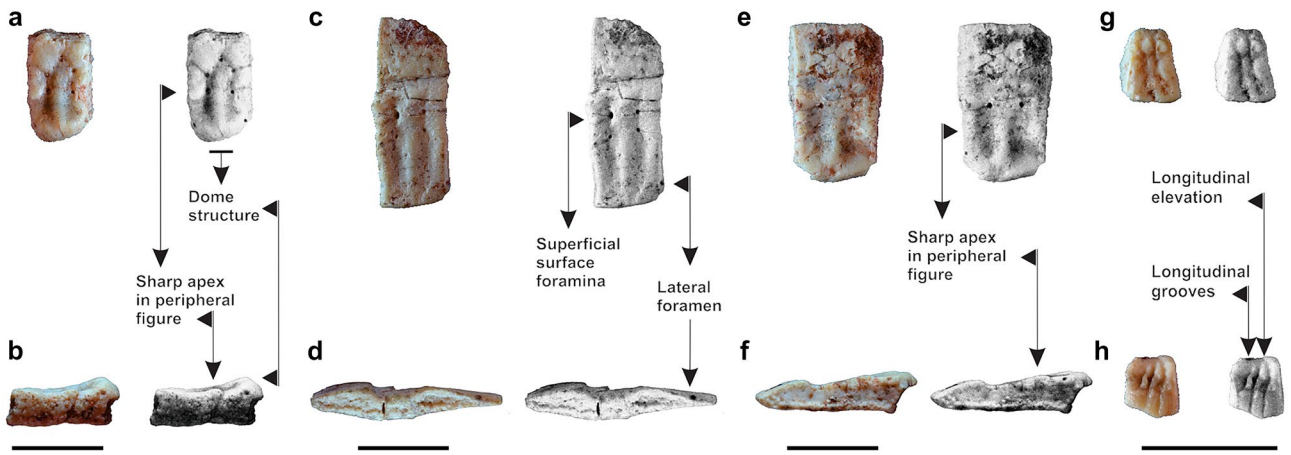


**Fig. 4** *Noatherium emilioi*, gen. et sp. nov. IBIGEO-P 75: (**a**) external surface of the movable osteoderm of the movable band; (**b**) lateral surface of the movable osteoderm of the movable band. IBIGEO-P 74: (**c**) external surface of the semifixed osteoderm of the pelvic buckler; (**d**) lateral surface of the semifixed osteoderm of the pelvic buckler. IBIGEO-P 72: (**e**) lateral surface of the fixed osteoderm of the dorsal carapace. Pucatherium parvum IBIGEO-P 121: (**f**) external surface of the movable osteoderm of the movable band. IBIGEO-P 121: (**g**) external surface of the fragment of a movable osteoderm of the movable band. Scale bars = 10 mm

individual. For this reason, we consider these specimens as holotype and paratypes.

**Diagnosis** Osteoderm with a conspicuous central keel that does not reach the posterior edge of the osteoderm is present in the midline of the lageniform figure. The external surface of the peripheral figures rises towards its caudal portion culminating in an external markedly sharp apex. The posterior portion of the external surface of the fixed osteoderm is very strongly elevated, surpassing the height of the medial keel, and delimiting a dome structure. The piliferous system is restricted to only one small foramen on each lateral margin. The posterior and lateral contact surfaces between the osteoderms are smooth.

**Description** The external surface of the osteoderms is smooth. The fixed osteoderms have a principal lageniform figure that occupies the posterior three-quarters of the external surface of the osteoderm (Fig. 4a, b). The neck of this figure represents half of its length. Four peripheral figures, two anterior and two lateral, delimited by weakly marked sulci, surround the anterior portion of the lageniform figure. On the external surface, five well-developed foramina are present in the intersection of the sulci that delimit the anterior and lateral peripheral figures from the principal one. The external surface of the anterior peripheral figures is flat, whereas this surface rises towards its caudal portion culminating in an external markedly sharp apex in the lateral peripheral figures, while in *Parutaetus* Ameghino, 1902, all peripheral figures are convex. A conspicuous central keel that does not reach the posterior edge of the osteoderm is present in the midline of the lageniform figure. The central keel has its edges parallel, while this edge gradually or abruptly converges towards the posterior border in *Parutateus* (Ciancio et al. 2016). The posterior portion of the osteoderm is very strongly elevated, surpassing the height of the central keel, and delimiting a dome structure, which is a unique feature among the armadillos (Fig. 4b). The piliferous system is poorly developed; it includes only one small foramen on each lateral margin, near to the posterior border, while in *Parutaetus* and *Punatherium catamarquensis* Ciancio et al., 2016, small piliferous foramina are present in the posterior margin (Ciancio et al. 2016). The anterior, posterior, and lateral contact surfaces between the osteoderms are smooth, while as shown by Ciancio et al. (2013), these show well-developed protuberances in *Parastegosimpsonia peruana* Ciancio et al., 2013.

The articular region of the movable osteoderms occupies one-third of it (Fig. 4c, d). As in most armadillos, this region is smooth, while in *Pucatherium parvum* Herrera et al., 2012, there are two to three marked longitudinal elevations, separated by deep grooves (Herrera et al. 2012, 2019). The exposed external surface of the osteoderm has a slightly marked principal lageniform figure that occupies almost the complete exposed external surface of the posterior portion of the osteoderm. The neck of this figure represents one-third of its length and is surrounded by four small peripheral figures, two anterolateral and two lateral, which are delimited by slightly marked sulci. On the external surface, four small foramina are present; these foramina are located in the intersection of the sulci that delimit them from the central one. The external surface of the lateral peripheral figures rises towards its caudal portion culminating in an external slightly sharp apex. A central keel that does not reach the posterior edge of the osteoderm is present in the midline of the lageniform figure. The central keel has parallel edges. The piliferous system is poorly developed and restricted to the lateral margin, while in *Lumbreratherium oblitum*, few piliferous foramina are present in the posterior margin of the osteoderm (Herrera et al. 2016). There is only one small foramen on each side, positioned near the posterior margin of the osteoderm. The posterior and lateral contact surfaces between the osteoderms are smooth.

The articular region of the semifixed anterior osteoderm of the pelvic buckler occupies one-third of it (Fig. 4e, f). The exposed external surface of the osteoderm has a principal lageniform figure that occupies the posterior three-quarters of the exposed external surface of the osteoderm. The neck of this figure represents half its length. Two anterolateral peripheral figures, delimited by weakly marked sulci, surround the lateral portion of the neck. On the external surface, four well-developed foramina are present; the posterior ones are located in the intersection of the sulci that delimit the anterolateral peripheral figures from the principal one. The external surface of the anterolateral peripheral figures rises towards its caudal portion culminating in a markedly sharp external apex. A clear central keel that does not reach the posterior edge of the osteoderm is present in the midline of the posterior part of the lageniform figure. The central keel has parallel edges. The posterior portion of the osteoderm is at the same level as the central keel. The piliferous system is poorly developed and restricted to the lateral margin. There is only one small foramen on each side, positioned near to the posterior margin of the osteoderm. The posterior and lateral contact surfaces between the osteoderms are smooth.

**Measurements** *Noatherium emilioi* is a medium-size armadillo. The measurements of the fixed osteoderm are 7.52 mm in width, 12.15 mm in length, and 4.98 mm in thickness; of the movable osteoderm are 7.63 mm in width, 21.11 mm in length, and 3.10 mm in thickness; and the semifixed anterior osteoderm are 10.49 mm in width, 17.87 mm in length, and 4.50 mm in thickness.

**Remarks.** The presence of smooth lateral walls, foramina on the lateral edges, and smooth external surface would indicate a similarity with Astegotheriinae. However, unlike

the latter, in which the osteoderms are thin and the figures are weakly delimited, in the new taxon, the thickness of the osteoderms of comparable areas is much greater, and has well-defined figures similar to that observed in euphractines. This peculiar combination of features prevents us from making a suprageneric taxonomic assignment.

*Pucatherium* Herrera et al., 2012

**Type and Only Species** *Pucatherium parvum*; southeast of Sierra Aguilar, 23°16'8.51" S 65°33'21.66" W, Humahuaca Department, Jujuy Province, Argentina; Casa Grande Formation.

*Pucatherium parvum* Herrera et al., 2012
(Fig. 4g, h)

**Type Specimen** PVL 6398, 74 dorsal carapace osteoderms.

**Geographic and Stratigraphic Occurrence** Antofagasta de la Sierra, Catamarca Province, Argentina, middle member of Geste Fm. (Ciancio et al. 2016); Quebrada El Paso, near Pozuelos salt flat, Los Andes Department, Salta Province, Argentina, middle member of Geste Fm. (Ciancio et al. 2016); Juramento River, La Viña Department, Salta Province, Argentina; upper section of the Lumbrera Fm. (Herrera et al. 2019); Cerro TinTin, Cachi Department, Salta Province, Argentina, Quebrada de los Colorados Fm. (Ciancio et al. 2016). Laguna and Casa Grande rivers, southeast of Sierra Aguilar, Jujuy Province, Argentina, Casa Grande Fm. (Ciancio et al. 2016); Camino de Los Colorados, Los Cardones National Park, Salta Province, Argentina, Quebrada de Los Colorados Fm., Los Cardones National Park, Calchaquí Valleys, Salta Province, Argentina, lower section of the Lumbrera Fm. (this work).

**Referred Material** IBIGEO-P 121, four osteoderms. IBIGEO-P 126, one osteoderm.

**Description** The following combination of osteoderm features allows us to assign these osteoderms to *Pucatherium parvum*. The external articular surface of the anterior part shows two or three well-developed longitudinal crests, separated by deep grooves. The external surface of the posterior part of the osteoderm is slightly wrinkled, with a principal central figure, surrounded by lateral grooves, roughly rectangular and with rounded corners.

The specimen IBIGEO-P 126 is complete and its measurements are 3.12 mm in width, 5.46 mm in length, and 1.56 mm in thickness. Other specimens recovered a few meters from the former show measurements that vary from 3.62 to 5.46 mm in width and 5.06 to 8.61 mm in length, and 1.65 to 1.73 mm in thickness. These ranges in the measurement of osteoderms are within the variation reported for this species. According to Herrera et al. (2012), the osteoderms of the type specimen (PVL 6398) are small; their measurements vary from 2.75 to 3.17 mm in width, 3.43 to 5.17 mm in length, and 1.09 to 1.89 mm in thickness. Herrera et al. (2019) reported the following range of measurements for the specimen PVL 6384: 4.07 to 5.58 mm in width, and 4.82 to 9.60 mm in length.

**Remarks.** According to Herrera et al. (2016), *Pucatherium parvum* and *Lumbreratherium oblitum* constitute a natural group that is located in a basal position within the Dasypodidae -clade that for these authors is formed by all cingulates except *Peltephilus* Ameghino, 1887- with only *L. oblitum* present in the lower section of the Lumbrera Fm.

## Chronostratigraphy: U-Pb Age

The analyzed sample LSLF-ELF1, obtained from a paleosol level located inside the Faja Verde in the LSLF at 10 m below the contact with the Casa Grande Fm. (Fig. 1c) in the Tres Cruces section (Jujuy Province), gave an average age of 46.2 ± 7.3 Ma (MSWD = 1.3, 95 % confidence) (Fig. 3). We chose to report the isochron age instead of a multiple U-Pb ages because of the relatively low concentrations in U in the sample as well as the moderate U/Pb ratios, and its expected young age. The isochron technique has generally provided better results for Cenozoic carbonates (Tamayo Silva et al. 2012).

## Discussion and Conclusions

### Geochronology

The new U-Pb age of 46.2 ± 7.3 Ma presented here for the top of the LSLF has important implications for the chronostratigraphy and the faunal content of the unit. The top of the LSLF is now placed at the base of the Lutetian (middle Eocene); thus, most of the section must have been deposited during the Ypresian age (early Eocene). This date contradicts the age model of del Papa et al. (2010) in which the base of the LSLF is around 46 Ma and the section is almost entirely included in the Lutetian age (Fig. 5). In the same manner, the age of 54.5 Ma for the top of the LSLF (Sempere et al. 1997) is no longer applicable. On the contrary, the radioisotopic date presented here agrees with the age model of White et al. (2018) based on the magnetostratigraphy of the underlying Maíz Gordo Fm., which set the top of the Maíz Gordo Fm. to the Thanetian-Ypresian boundary (Paleocene–Eocene), and the base of the Lumbrera Fm. to the early Eocene (Ypresian). In addition, our results significantly support the paleoclimatic reconstruction of Andrews et al. (2017). As mentioned above,

these authors correlated, preferentially, the isotopic excursion registered at the base of the LSLF to the early Eocene global events EECO and ETM2 defined by Zachos et al. (2001, 2008, 2010). Thus, the Ypresian-early Lutetian age for the LSLF is supported by multi-proxy evidence including radio-isotopic dates (this work), magnetostratigraphy (White et al. 2018), and hyperthermal correlations (Andrews et al. 2017).

With respect to our fossiliferous levels, we mentioned that we worked on the same levels as Andrews et al. (2017) in the Tin Tin section. They recorded in this site the early Eocene hyperthermal events in the first 150 m of the LSLF (Fig. 1b). Our fossils come from 100 m above the base of the LSLF, so they are entirely included in the hyperthermal span, and, consequently, its age could be limited to the interval 52–55 Ma, which is the chronology defined by Zachos et al. (2008) for the EECO and ETM2.

## Biochronology

Traditionally, the vertebrate fauna recovered from the lower section of the Lumbrera Fm. was chronologically assigned to the Casamayoran SALMA based on the similar 'evolutionary stage' that this assemblage shared with the Casamayoran SALMA in Patagonia (Carbajalet al. 1977; Pascual 1980a, b; Pascual et al. 1981; Bond and Vucetich 1983), which by that time was referred to the early Eocene (e.g., Pascual et al. 1965; Marshall et al. 1983). At present, the Casamayoran SALMA is subdivided into the Barrancan and Vacan subages (Cifelli 1985; Carlini et al. 2010; Woodburne et al. 2014;

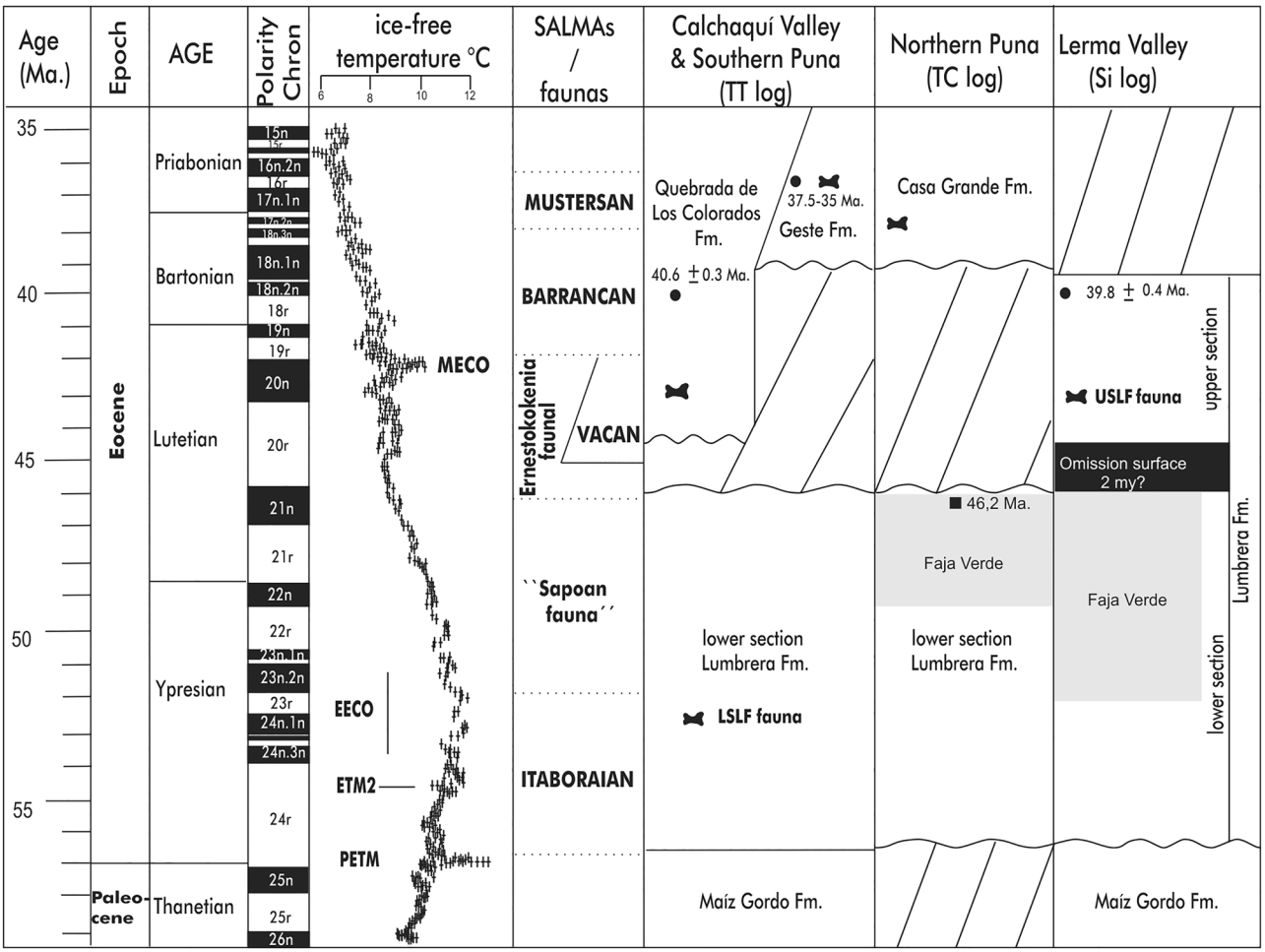


**Fig. 5** Late Paleocene-Eocene time scale showing South American mammalian biochronological units. Age, Epoch, Stage, and Polarity Chron follow Ogg (2012). Age of the Patagonian units follows Krause et al. (2017). Black circles represent the known isotopic dates based on: del Papa et al. (2010) (upper section of the Lumbrera Fm.). Stratigraphy of Bolivia follows DeCelles and Horton (2003) and Horton (2018); northwestern Argentina follows White et al. (2018) and partially del Papa et al. (2010). Black squares represent age presented in this work on the upper levels of the lower section of the Lumbrera Fm. Arrows in the South American mammalian assemblages column highlight the location of northwestern Argentina faunas. Age of Paso del Sapo fauna follows Tejedor et al. (2009). Bones represent the mammal-bearing levels

Krause et al. 2017). The former subage has been positioned by Dunn et al. (2013) between 41.7 and 39 Ma (Bartonian), whereas the latter between 44 and 46 Ma (Lutetian) (Madden et al. 2005; Ré et al. 2005, 2010a, b; and see Woodburne et al. 2014 and papers cited therein). According to different authors, the fossiliferous levels of the lower section of the Lumbrera Fm. are equivalent to the Vacan Subage (del Papa et al. 2010; Powell et al. 2011; García-López et al. 2019). However, this biochronology is not supported by the absolute dating provided in this work. The top of the LSLF is now established by radioisotopy at 46. 2 ± 7.3 Ma (early Lutetian), and the record of the EECO and ETM2 in the first 150 m of the LSLF set the initial deposition of the section in the early Eocene (early Ypresian). With these new constraints, the species based on specimens recovered on the lower levels of the LSLF (this work) are chronologically equivalent to the Itaboraian SALMA (56.1–51.4 Ma; Woodburne et al. 2014; Krause et al. 2017). In addition, the species based on specimens collected from the top of the section (Faja Verde: 46.2 Ma) could have been coeval to the 'Sapoan' fauna (Patagonia) and La Meseta (Antarctica) (Woodburne et al. 2014) and partially to the *Ernestokokenia* faunal zone (Krause et al. 2017).

Regarding the spatiotemporal distribution of the early Eocene species, *Noatherium emilioi* is only represented in the lower levels of the LSLF (~ 52–55 Ma); *Pucatherium parvum* (taxon traditionally used as fossil guide for the middle Eocene of the NWA) is distributed in the basal levels of the LSLF (this work), the USLF, the Quebrada de los Colorados, and Geste formations (Herrera et al. 2019); whereas *Lumbreratherium oblitum*, not registered in the levels reported here, is present only in the LSLF, but the lack of precise stratigraphic data does not allow us to refine its temporal range within this formation (~ 53–46 Ma). According to the geochronological synthesis presented by Chornogubsky et al. (2019) for the Paleogene of the NWA, the USLF, dated at El Simbolar, are similar in age to those from the Quebrada los Colorados Fm. at Los Cardones National Park (older than 39.9 Ma; DeCelles et al. 2011), while the middle levels from the Geste Fm. that contains the fossils are considerably younger, being ca. 37–35 Ma in age (DeCelles et al. 2007). In this context, the biochron of *Pucatherium parvum* extends for at least 16 Ma (Fig. 5), therefore, excluding it as a fossil guide for the middle Eocene as it was previously conceived (e.g., Herrera et al. 2019).

## Carapace Cingulate Evolution

In this new geochronological scheme, the cingulate fauna from the lower levels of the LSLF and the Itaboraí Fm. (Brazil) are the oldest ones in America. The Itaboraian SALMA was defined based on the latter formation, and it was first considered late Paleocene (Cifelli 1983; Oliveira and Bergqvist 1998; Bergqvist et al. 2004), and, more recently, early Eocene (Woodburne et al. 2014). The confrontation of the cingulate taxa of the base of the LSLF with the only cingulate of the Itaboraí Fm., *Riostegotherium yanei*, shows that these units share neither genus nor species. At a supra-generic level, it is also not possible to establish any kind of relationship between both cingulates faunas, because this type of assignment is uncertain for the taxa of the LSLF, and, recently, the assignment of *Riostegotherium yanei* within the Astegotheriini has been questioned (Bergqvist et al. 2019). Traditionally, this species has been related to the Paleogene Astegotheriini Dasypodinae, but a recent study of the internal morphology of its osteoderms suggests a greater similarity with those osteoderms of the living species *Dasypus novemcinctus* Linnaeus, 1758 (Dasypodini Dasypodinae) (Bergqvist et al. 2019).

The new taxonomic cingulate association of the lower levels of the LSLF (*Noatherium* and *Pucatherium*) shows osteoderms with smooth lateral surfaces. This feature allows us to infer the presence of an exoskeleton with a high degree of lateral mobility between osteoderms. This feature was originally described for *Riostegotherium yanei* (Oliveira and Bergqvist 1998), but recently the lateral surfaces of the osteoderms of this taxon were described as rough and this fact was interpreted as evidence of firm sutures between them (Bergqvist et al. 2019).

With respect to the general morphology of the carapace, Herrera et al. (2019) described a large portion of a carapace of *Pucatherium* in which only movable bands of osteoderms are recorded; according to these authors, this was considered a specific diagnostic feature. With respect to *Noatherium*, the presence of the anterior semifixed osteoderm of the pelvic buckler, fixed, and movable osteoderms allows us to recognize a carapace model formed by a sector with movable transverse osteoderm bands, and another sector formed by a pelvic shield. Unfortunately, there is no conclusive evidence of the existence of a scapular shield, because it is not possible to establish if the fixed osteoderm described here corresponds to the scapular or the pelvic shield of the carapace. Finally, according to Bergqvist et al. (2019), the carapace of *Riostegotherium yanei* is composed of transverse movable bands and two carapace shields (scapular and pelvic). In this context, two (and perhaps three) of the five carapace models listed for Cingulata by Fernicola et al. (2018) (Fig. 6a-e) are present in early Eocene times: (1) cranial osteoderms forming a scapular shield separated from the pelvic shield by transverse movable bands crossing the carapace form side to side (e.g., *Riostegotherium*, possibly *Noatherium*, *Tolypeutes* Illiger, 1811, and *Dasypus* Linnaeus, 1758) (Fig. 6a); (2) osteoderms of the carapace forming transverse movable bands that occupy the whole carapace (e.g., *Pucatherium*, *Stegotherium* Ameghino, 1887, and

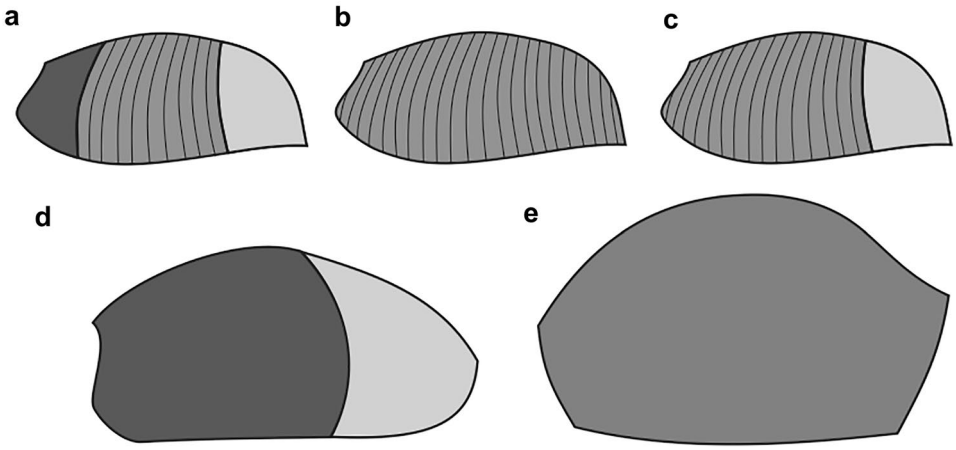


**Fig. 6** Dorsal carapace models. (**a**) Scapular shield separated from the pelvic shield by transverse movable bands crossing the carapace from side to side; (**b**) Osteoderms forming transverse movable bands that occupy the whole carapace; (**c**) Caudal osteoderms forming a pelvic shield, which is preceded by transverse movable bands crossing the carapace from side to side over the lumbar and thoracic regions of the vertebral column; (**d**) Carapace formed by two large pelvic and scapular shields overlapping each other without separate transverse movable band(s); (**e**) Osteoderms articulate with each other forming an undivided carapace without separate shields or transverse movable bands crossing the carapace from side to side

*Peltephilus*) (Fig. 6b); and possibly (3) caudal osteoderms forming a pelvic shield, which are preceded by transverse movable bands crossing the carapace from side to side over the lumbar and thoracic regions of the vertebral column (e.g., possibly *Noatherium*, *Proeutatus* Ameghino, 1891) (Fig. 6c). The remaining two models, absent in these levels, correspond to the one of glyptodonts, which show osteoderms that articulate with each other forming an undivided carapace without separate shields or transverse movable bands crossing the carapace from side to side (Fig. 6d); and the other of a peculiar group known as Pachyarmatheriidae with the carapace formed by two large pelvic and scapular shields overlapping each other without separate transverse movable band(s) (Fig. 6e).

The presence of at least three taxa of cingulates (*Riostegotherium*, *Noatherium*, and *Pucatherium*), a number that could rise to four (*Lumbreratherium*), in the early Eocene of South America (ca. 52–55, during the EECO), shows an earlier diversification of the cingulates than previously recognized. This early diversification also supported by the wide geographical distribution of this fauna (the outcrops of Brazil and Argentina are located more 2000 km from each other, and both are very close to the Tropic of Capricorn), the morphological diversity in the carapace models, and the lateral mobility of the osteoderms. This scheme is in line with the oldest values of the diversification ranges provided by different molecular studies that are positioned between 49.1 and 52.1 (Delsuc et al. 2004, 2012; Gibbs et al. 2016). Thus, this new early Eocene cingulate scenario supports a Paleocene (and perhaps even Late Cretaceous) diversification for the Cingulata. Thus, the basal phylogenetic position of *Pucatherium* and *Lumbreratherium* within this clade (Herrera et al. 2016), and the fact that the earliest records of Cingulata in high latitudes (e.g., Patagonia, Argentina) correspond to late early to middle Eocene (Gaudin and Croft 2015; Woodburne et al. 2014) reinforce the hypothesis of an intertropical origin of this clade (see Gaudin and Croft 2015 and papers cited therein).

**Acknowledgements** We thank the rangers of the Los Cardones National Park and Administración de Parques Nacionales (APN) for their logistic support of our fieldwork. We also thank Comisión Nacional de Energía Atómica (CNEA) for providing the facilities of the Don Otto camp. We are grateful to the curators M. Reguero (MLP), Pablo Ortiz (PVL), and former curator A. Kramarz (MACN) for making available the collections under their care. This is a contribution to projects Agencia Nacional de Promoción Científica y Tecnológica (ANPYCT) grant PICT 201–0508 to N. Zimicz, L. Chornogubsky, J.C. Fernicola, M. Arnal, and M. Bond; CONICET-MACN grant PUE22920160100098 to L. Chornogubsky and J.C. Fernicola; and IBIGEO-PUE to N. Zimicz. M.N.D. acknowledges support from the Romanian Executive Agency for Higher Education, Research, Development and Innovation Funding project PN-III-P4-ID-PCCF-2016-0014.

## References

Andrews E, White T, del Papa C (2017) Paleosol-based paleoclimate reconstruction of the Paleocene-Eocene Thermal Maximum, northern Argentina. Palaeogeogr Palaeoclimatol Palaeoecol 471:181–195

Barbeau DL Jr, Ducea MN, Gehrels GE, Kidder S, Wetmore PH, Saleeby JB (2005) U-Pb detrital-zircon geochronology of northern Salinian basement and cover rocks. Geol Soc Am Bull 117:466–481

Bergqvist LP, Abrantes EAL, Avilla LS (2004) The Xenarthra (Mammalia) of São José de Itaboraí Basin (upper Paleocene, Itaboraian), Rio de Janeiro, Brazil. Geodiversitas 26:323–337

Bergqvist LP, Pereira PVLGC, Machado AS, Castro MC, Melki LB, Lopes RT (2019) Osteoderm microstructure of *Riostegotherium yanei*, the oldest Xenarthra. An Acad Bras Cienc 91:e20181290

Bond M, Vucetich MG (1983) *Indalecia grandesis* gen. et sp. nov. del Eoceno temprano del Noroeste Argentino, tipo de una nueva subfamilia de los Adianthidae (Mammalia, Litopterna). Rev Asoc Geol Arg 37:107–117

Carbajal E, Pascual R, Pinedo R, Salfity J, Vucetich MG (1977) Un nuevo mamífero de la Formación Lumbrera (Grupo Salta) de la comarca de Carahuasi (Salta, Argentina). Edad y correlaciones. Publicaciones del Museo Municipal de Ciencias Naturales de Mar del Plata "Lorenzo Scaglia" 2:148–163

Carlini AA, Ciancio MR, Scillato-Yané GJ (2010) Middle Eocene–early Miocene Dasypodidae (Xenarthra) of southern South America: faunal succession at Gran Barranca–biostratigraphy and paleoecology. In: Madden RH, Carlini AA, Vucetich MG, Kay RF (eds) The Paleontology of Gran Barranca: Evolution and Environmental Change through the Middle Cenozoic of Patagonia. Cambridge University Press, Cambridge, pp 106–129

Chornogubsky L, Zimicz AN, Goin FJ, Fernicola JC, Payrola P, Cárdenas M (2019) New Palaeogene metatherians from the Quebrada de Los Colorados Formation at Los Cardones National Park (Salta Province, Argentina). J Syst Palaeontol 17:539–555

Ciancio MR, Carlini AA, Campbell KE Jr, Scillato-Yané GJ (2013) New Paleogene cingulates (Mammalia, Xenarthra) from Santa Rosa, Peru, and their importance in the context of South American faunas. J Syst Palaeontol 11:727–741

Ciancio MR, Herrera C, Aramayo A, Payrola P, Babot J (2016) Diversity of cingulates (Mammalia, Xenarthra) in the middle–late Eocene of northwestern Argentina. Acta Palaeontol Pol 61:575–590

Cifelli RL (1983) Eutherian tarsals from the late Paleocene of Brazil. Am Mus Novitates 2761:1–31

Cifelli RL (1985) Biostratigraphy of the Casamayoran, early Eocene of Patagonia. Am Mus Novitates 2820:1–26

DeCelles PG, Carrapa B, Gehrels GE (2007) Detrital zircon U-Pb ages provide provenance and chronostratigraphic information from Eocene synorogenic deposits in northwestern Argentina. Geology 35:323–326

DeCelles PG, Carrapa B, Horton BK, Gehrels GE (2011) Cenozoic foreland basin system in the central Andes of northwestern Argentina: implications for Andean geodynamics and modes of deformation. Tectonics 30:TC6013. https://doi.org/10.1029/2011TC002948

DeCelles PG, Horton BK (2003) Early to middle Tertiary foreland basin development and the history of Andean crustal shortening in Bolivia. Geol Soc Am Bull 115(1):58–77. https://doi.org/10.1130/0016-7606(2003)115<0058:ETMTFB>2.0.CO;2

del Papa CE (2006) Estratigrafía y paleoambientes de la Formación Lumbrera, Grupo Salta, noroeste argentino. Rev Asoc Geol Arg 61:15–29

del Papa CE, Hongn F, Payrola Bosio P, Powell J, Deraco V, Herrera C (2013) Relaciones estratigráficas de las formaciones quebrada de los colorados y angastaco (paleógeno-neógeno), Valles calchaquíes, Salta (Argentina): significado en el análisis de la cuenca del grupo Payogastilla. Lat Am J Sedimentol Basin Anal 20:51–64

del Papa CE, Kirshbaum A, Powell JE, Brod A, Hongn F, Pimentel M (2010) Sedimentological, geochemical and paleontological insights applied to continental omission surfaces: a new approach for reconstructing an Eocene foreland basin in NW Argentina. J S Am Earth Sci 29:327–345

Delsuc F, Gibb GC, Kuch M, Billet G, Hauthier L, Southon J, Roullard J, Fernicola JC, Vizcaíno SF, MacPhee RDE, Poinar H (2016) The phylogenetic affinities of the extinct glyptodonts. Curr Biol 26(4):R155–R156

Delsuc F, Superina M, Tilak MK, Douzery EJ, Hassanin A (2012) Molecular phylogenetics unveils the ancient evolutionary origins of the enigmatic fairy armadillos. Mol Phylogenet Evol 62:673–680

Delsuc F, Vizcaíno SF, Douzery D (2004) Influence of Tertiary paleoenvironmental changes on the diversification of South American mammals: a relaxed molecular clock study within xenarthrans. BMC Evol Biol 4:11

Ducea MN, Ganguly J, Rosenberg EJ, Patchett PJ, Cheng W, Isachsen C (2003) Sm–Nd dating of spatially controlled domains of garnet single crystals: a new method of high-temperature thermochronology. Earth Planet Sci Lett 213:31–42

Dunn ER, Madden RH, Kohn MJ, Schmitz MD, Strömberg CAE, Carlini AA, Ré GH, Crowley J (2013) A new chronology for middle Eocene–early Miocene South American Land Mammal Ages. Geol Soc Am Bull 125:539–555

Fernández M, Zimicz N, Bond M, Chornogubsky L, Arnal M, Cárdenas M, Fernicola JC (2021) New Palaeogene South American native ungulates from the Quebrada de los Colorados Formation at Los Cardones National Park, Salta Province (Argentina). Acta Palaeontol Pol 66:85–97

Fernicola JC, Porpino KO (2012) Exoskeleton and systematics: a historical problem in the classification of glyptodonts. J Mammal Evol 19:171–183

Fernicola JC, Rinderknecht A, Jones W, Vizcaíno SF, Porpino K (2018) A new species of *Neoglyptatelus* (Mammalia, Xenarthra, Cingulata) from the late Miocene of Uruguay provides new insights on the evolution of the dorsal armor in cingulates. Ameghiniana 55:233–252

Fernicola JC, Vizcaíno SF (2008) Revisión del género *Stegotherium* Ameghino, 1887 (Mammalia, Xenarthra, Dasypodidae). Ameghiniana 45:321–332

Fernicola JC, Vizcaíno SF (2019) Cingulates (Mammalia, Xenarthra) of the Santa Cruz Formation (early–middle Miocene) from the Río Santa Cruz, Argentine Patagonia. Publ Electron de la Asoc Paleontol Argentina 19:85–101

Francia A, Ciancio MR (2013) First record of *Chaetophractus villosus* (Mammalia, Dasypodidae) in the late Pleistocene of Corrientes Province (Argentina). Rev Mus La Plata 13:1–9

García-López A, Deraco V, Rougier GW, del Papa C, Babot J, Bertelli S, Herrera CM, Giannini NP (2019) New Record of *Pampahippus secundus* (Mammalia, Notoungulata) from the Upper Lumbrera Formation, Eocene of northwestern Argentina. J Vertebr Paleontol. https://doi.org/10.1080/02724634.2019.1582537

Gaudin TJ (1999) The morphology of the xenarthrous vertebrae (Mammalia, Xenarthra). Fieldiana Geol 41:1–38

Gaudin TJ, Croft DA (2015) Paleogene Xenarthra and the evolution of South American mammals. J Mammal 96:622–634

Gibbs GC, Condamine FL, Kuch M (2016) Shotgun mitogenomics provides a reference phylogenetic framework and timescale for living xenarthrans. Mol Biol Evol 33:621–642

Herrera CMR, Esteban GI, Ciancio MR, del Papa C (2019) New specimen of *Pucatherium parvum* (Xenarthra, Dasypodidae), a singular dasypodid of the Paleogene (Eocene) of northwest Argentina: importance in the early evolution of armadillos. J Vertebr Paleontol. https://doi.org/10.1080/02724634.2019.1670669

Herrera CMR, Powell JE, del Papa CE (2012) Un nuevo Dasypodidae (Mammalia, Xenarthra) de la Formación Casa Grande (Eoceno) de la provincia de Jujuy, Argentina. Ameghiniana 49:267–271

Herrera CMR, Powell JE, Esteban GI, del Papa C (2016) A new Eocene dasypodid with caniniforms (Mammalia, Xenarthra, Cingulata) from northwest Argentina. J Mammal Evol. https://doi.org/10.1007/s10914-016-9345-x

Horton BK (2018) Sedimentary record of Andean mountain building. Earth-Sci Rev 178:279–309. https://doi.org/10.1016/j.earscirev.2017.11.025

Krause JM, Clyde WC, Ibañez-Mejía M, Schmitz M, Barnum T, Bellosi E, Wilf P (2017) New age constraints for early Paleogene strata of central Patagonia, Argentina: implications for the tim-

ing of South America Land Mammal Ages. Geol Soc Am Bull 129:886–903
Krmpotic CM, Ciancio MR, Barbeito C, Carlini AA (2009) Osteoderm morphology in recent and fossil euphractinae xenarthrans. Acta Zool 90:339–351
Ludwig KR (2012) User's manual for Isoplot version 3.75–4.15: a geochronological toolkit for Microsoft Excel. Berkeley Geochronological Center Special Publication 5
Madden RH, Kay RF, Heizler M, Vilas J, Ré GH (2005) Geochronology of the Sarmiento Formation at Gran Barranca and elsewhere in Patagonia: calibrating Middle Cenozoic mammal evolution in South America. Actas de XVI Congr Geol Argent 4:411–412
Marquillas R, del Papa C, Sabino I (2005) Sedimentary aspects and paleoenvironmental evolution of a rift basin: Salta Group (Cretaceous-Paleogene), northwestern Argentina. Int J Earth Sci 39:489–516
Marshall LG, Muizon C de, Sigé B (1983) Late Cretaceous mammals (Marsupialia) from Bolivia. Geobios 16:739–745
McDonald HG (2018) An overview of the presence of osteoderms in sloths: implications for osteoderms as a plesiomorphic character of the Xenarthra. J Mammal Evol 25:485–493
Meredith RW, Janečka JE, Gatesy J, Ryder OA, Fisher CA, Teeling EC, Goodbla A, Eizirik E, Taiz LLS, Stadler T, Rabosky DL, Honeycutt RL, Flynn JJ, Ingram CM, Steiner C, Williams TL, Robinson TJ, Burk-Herrick A, Westerman M, Ayoub NA, Springer MS, Murphy WJ (2011) Impacts of the Cretaceous terrestrial revolution and KPg extinction on mammal diversification. Science 334:521–524
Oliveira EV, Bergqvist LP (1998) A new Paleocene armadillo (Mammalia, Dasypodoidea) from the Itaboraí basin, Brazil. In: Publicación Especial 5: Paleógeno de América Argentina y de la Península Antártica. Asociación Paleontológica Argentina, Buenos Aires, pp 35–40
Pascual R (1980a) Nuevos y singulares tipos ecológicos de marsupiales extinguidos de América del Sur (Paleoceno Tardío o Eoceno Temprano) del Noroeste Argentino. Actas I Congreso Argentino de Paleontología y Bioestratigrafía, Buenos Aires, Asoc Paleontol Argentina 2:151–173
Pascual R (1980b) Prepidolopidae, nueva familia de Marsupialia Didelphoidea del Eoceno sudamericano. Ameghiniana 17:216–242
Pascual R, Bond M, Vucetich MG (1981) El Subgrupo Santa Bárbara (Grupo Salta) y sus vertebrados. Cronología paleoambientes y paleobiogeografía. VIII Congr Geol Argentino Actas 3:743–758
Pascual R, Ortega Hinojosa EJ, Gondar D, Tonni E (1965) Las edades del Cenozoico mamalífero de la Argentina, con especial atención a aquellas del territorio Bonaerense. Anales de la Comisión de Investigaciones Científicas 6:165–193
Powell JE, Babot MJ, García-López DA, Deraco MV, Herrera C (2011) Eocene vertebrates of northwestern Argentina: annotated list. In: Salfity JA, Marquillas R (eds) Cenozoic Geology of the Central Andes of Argentina. SCS Publisher, Salta, pp 349–370
Ré GH, Bellosi ES, Heizler M, Vilas JF, Madden RH, Carlini AA, Kay RF, Vucetich MG (2010a) A geochronology for the Sarmiento Formation at Gran Barranca. In: Madden RH, Carlini AA, Vucetich MG, Kay RF (eds) The Paleontology of Gran Barranca. Cambridge University Press, Cambridge, pp 46–58
Ré GH, Geuna SE, Vilas JF (2010b) Paleomagnetism and magnetostratigraphy of Sarmiento Formation (Eocene-Miocene) at Gran Barranca, Chubut, Argentina. In: Madden RH, Carlini AA, Vucetich MG, Kay RF (eds) The Paleontology of Gran Barranca. Cambridge University Press, Cambridge, pp 32–45
Ré GH, Madden RH, Heizler M, Vilas JF, Rodríguez ME (2005) Polaridad magnética de las sedimentitas de la Formación Sarmiento (Gran Barranca de Lago Colhue Huapi, Chubut, Argentina). Actas XVI Congr Geol Argentino, La Plata 4:387–394
Sempere T, Butler RF, Richards DR, Marshall LG, Sharp W, Swisher CC III (1997) Stratigraphy and chronology of Upper Cretaceous–lower Paleogene strata in Bolivia and northwest Argentina. Geol Soc Am Bull 109:709–727
Silva-Tamayo JC, Ducea M, Cardona A, Montes C, Rincón D, Machado A, Flores A, Sial A, Pardo A, Niño H, Ramírez V, Jaramillo C, Zapata P, Barrios L, Rosero S, Bayona G, Zapata V (2012) Precise U-Pb dating of Cenozoic tropical reef carbonates: linking the evolution of Cenozoic Caribbean reef carbonates to climatic and environmental changes. European Geosciences Union (EGU) General Assembly, pp 6657. Accessed 22–27 April 2012. https://ui.adsabs.harvard.edu/abs/2012EGUGA.14.6657S/abstract
Tejedor MF, Goin FJ, Gelfo JN, López GM, Bond M, Carlini AA, Scillato-Yané GJ, Woodburne MO, Chornogubsky L, Aragón E, Reguero MA, Czaplewski NJ, Vincon S, Martin GM, Ciancio M (2009) New early Eocene mammalian fauna from western Patagonia, Argentina. Am Mus Novitates 3638:1–43
White T, del Papa C, Andrews E (2018) Chronostratigraphy of Paleogene strata, Salta Basin, northwestern Argentina: a reply to Hyland and Sheldon's comment. Palaeogeogr Palaeoclimatol Palaeoecol 511:643–645
Woodburne MO, Goin FJ, Bond M, Carlini AA, Gelfo JN, López GM, Iglesias A, Zimicz AN (2014) Paleogene land mammal faunas of South America: a response to global climatic changes and indigenous floral diversity. J Mammal Evol 21:1–73
Zachos JC, Dickens GR, Zeebe RE (2008) An early Cenozoic perspective on greenhouse warming and carbon-cycle dynamics. Nature 451:279–283
Zachos JC, McCarren H, Murphy B, Röhl U, Westerhold T (2010) Tempo and scale of late Paleocene and early Eocene carbon isotope cycles: implications for the origin of hyperthermals. Earth Planet Sci Lett 299:244–249
Zachos JC, Pagani M, Sloan L, Thomas E, Billups K (2001) Trends, rhythms, and aberrations in global climate 65 Ma to present. Science 292:686–693